

PHYSICAL REVIEW B

CONDENSED MATTER

THIRD SERIES, VOLUME 44, NUMBER 12

15 SEPTEMBER 1991-II

Ground-state phase diagram of the one-dimensional extended Hubbard model

Joel W. Cannon*

*Department of Physics and Materials Research Laboratory, University of Illinois at Urbana-Champaign,
1110 West Green St., Urbana, Illinois 61801*

Richard T. Scalettar

Department of Physics, University of California, Davis, Davis, California 95616

Eduardo Fradkin

*Department of Physics and Materials Research Laboratory, University of Illinois at Urbana-Champaign,
1110 West Green St., Urbana, Illinois 61801*

(Received 7 February 1991)

We study the ground-state phase diagram of the extended Hubbard model through the Lanczos method using change-density-wave order-parameter distribution functions and finite-size scaling. We confirm the presence of a tricritical point, and estimate the phase boundary to occur at $V=2.92\pm 0.04$ at $U=5.5$, and at $V=1.65^{+0.10}_{-0.05}$ at $U=3.0$. We estimate the tricritical point to occur above $U=3.5$. Despite the restriction to small lattices, the increased accuracy of the Lanczos approach appears to provide a more precise estimate of the phase boundary and tricritical point than use of the Monte Carlo simulation.

I. INTRODUCTION

The extended Hubbard model is a simple many-body model that has a rich phase structure. It consists of spin- $\frac{1}{2}$ fermions that may hop between sites on a lattice, and which interact with each other via on-site and nearest-neighbor potentials. It is given by the Hamiltonian

$$H = -t \sum_{i,\sigma} (C_{i,\sigma}^\dagger C_{i+1,\sigma} + C_{i+1,\sigma}^\dagger C_{i,\sigma}) + U \sum_i n_{i\uparrow} n_{i\downarrow} + V \sum_i n_i n_{i+1}, \quad (1)$$

$$n_i = n_{i\uparrow} + n_{i\downarrow}.$$

Here, $C_{i,\sigma}^\dagger$ and $C_{i,\sigma}$ are the creation and annihilation operators for a fermion of spin σ at the i th spatial site, $n_{i,\sigma} = C_{i,\sigma}^\dagger C_{i,\sigma}$ is the number operator, U is the on-site interaction strength, V is the nearest-neighbor interaction strength, and t is the hopping strength.

In this paper we are interested in the half-filled-band case, with $U, V > 0$. At $T=0$, this has two ordered phases: a charge-density-wave (CDW) phase and a spin-density-wave (SDW) phase. The CDW phase has a discrete symmetry, and exhibits true long-ranged order,

while the SDW phase has a continuous symmetry, and consequently, by the Mermin-Wagner theorem, cannot have true long-range order. Rather, it is a critical state in which the staggered spin-density correlation function decays algebraically. The important questions concerning the model are as follows: where is the boundary between the two phases located, and what is the nature of the transition between the two phases?

Monte Carlo simulation¹⁻³ indicates that the phase boundary occurs at values of V greater than the $U=2V$ values given by weak-coupling renormalization-group (RG) (Ref. 4) and Hartree-Fock⁵ calculations, and that the transition is second order for small values of the coupling constants and first for large values. Earlier RG and finite-size scaling calculations predicted the shift in the phase boundary, but not the tricritical behavior.^{6,7}

The Monte Carlo calculations were performed using the "checkerboard breakup" method of simulating fermions in one spatial dimension.⁸ While this method has been proven reliable, it suffers from statistical errors and slow convergence near the phase boundary. Further, there are uncertainties associated with extrapolating results calculated at finite temperature to $T=0$, and to zero value of the discretization step, $\Delta\tau = \beta/N$ (β is the inverse temperature and N is the time dimension of the lattice simulation). Therefore, it is desirable to study the

model by an independent method that is essentially exact, and explicitly works at zero temperature.

The paper is organized as follows. In Sec. II we review our numerical methods. In particular, we describe how we obtain the order-parameter distribution function. In Sec. III, we present the results of calculations to determine the phase boundary and tricritical point. These include results obtained from the order-parameter distribution function and finite-size scaling. We also compare the results of this Lanczos calculation with earlier results based on the Monte Carlo method by two of us. Section IV presents our conclusions.

II. COMPUTATIONAL METHOD

Our method is to obtain the ground-state wave vector (via the Lanczos method), and determine the phase diagram from the wave vector by analyzing the CDW order-parameter distribution function following the method of Ref. 3. In addition, we perform finite-size scaling of the CDW and SDW structure factors and the parameter g , which is related to the fourth-order cumulant of the distribution. We will now briefly describe our method of obtaining the wave vector and the order-parameter distribution using the Lanczos method.

A. Calculation of the ground-state wave function and the CDW order-parameter distribution function using the Lanczos method

The Lanczos method creates a tridiagonal matrix by successive applications of H to a starting wave vector ψ_1 . The beauty of the Lanczos method is that, while in principle the tridiagonal matrix should have a dimension equal to the size of the basis, the principal eigenvalue can be accurately calculated after a much smaller number of applications of H .⁹⁻¹¹ Thus, we can obtain the ground-state energies to problems with very large bases by diagonalizing moderate-size matrices. For example, we found that 20 applications of H were sufficient to obtain the ground-state energy to six decimal places in a Hilbert space whose dimension was nearly 10^6 .

We would also like to obtain the ground-state eigenvector. Often, memory limitations make it difficult to obtain the eigenvector in a Lanczos calculation. The vectors of the tridiagonal basis, ψ_i , are normally discarded after being used in the calculation to save computer memory. To understand why this is done, consider the fact that each ψ_i has a number of components i equal to the total number of states in the Hilbert space. This is $\binom{N}{N/2}^2$, or 853 776 for $N=12$. Thus, storing the ψ_i would require about one-million words storage per application of the Hamiltonian, which very quickly exceeds most computer memories. One method to overcome this and obtain the eigenvector is the “modified Lanczos algorithm” of Dagotto *et al.*,¹² which diagonalizes after two applications of the Hamiltonian, and repeats the procedure using the eigenvector obtained in the diagonalization as the new starting wave vector. However, we found the “two-pass” method described below to be less susceptible to numerical instabilities, and to converge faster than

“modified Lanczos.”

We make two passes through the Lanczos algorithm. In the first, we obtain the ground-state energy, and the components α_i in the expansion of the ground-state wave vector Ψ_0 ,

$$\Psi_0 = \sum_i \alpha_i \psi_i \quad (2)$$

in the tridiagonal basis ψ_i . In the second, we explicitly construct Ψ_0 by sequentially recreating the ψ_i and performing one term of the sum in Eq. (2) at each step. This allows us to express the ground-state eigenvector in terms of our basis vectors with only a small increase in memory over that needed to obtain the ground-state energy. The cost of this is that our computation time is doubled. However, since Lanczos calculations are normally memory intensive rather than time intensive, this is acceptable.

B. Determining the CDW order-parameter distribution using the Lanczos algorithm

The CDW order parameter $m_0 = \sum_i \langle \Psi_0 | (-1)^i n_i | \Psi_0 \rangle = \langle \Psi_0 | \hat{m} | \Psi_0 \rangle$ of the ground-state wave function has a unique value (aside from degeneracies). However, within the real-space (or occupation number) basis that we do our calculations, we may think of it as being the sum over a distribution of possible values of m :

$$m_0 = \langle \Psi_0 | \hat{m} | \Psi_0 \rangle, \quad (3)$$

$$= \sum_{i,j} \langle \Psi_0 | \phi_i \rangle \langle \phi_i | \hat{m} | \phi_j \rangle \langle \phi_j | \Psi_0 \rangle, \quad (4)$$

$$= \sum_i |\langle \Psi_0 | \phi_i \rangle|^2 m_i. \quad (5)$$

In these equations, we made use of the fact that \hat{m} is diagonal ($\langle \phi_i | \hat{m} | \phi_j \rangle = m_i \delta_{i,j}$). Defining

$$P(m) = \sum_k |\langle \Psi_0 | \phi_k \rangle|^2 \delta_{m_k, m} \quad (6)$$

allows us to rewrite the sum as

$$m_0 = \sum_m m P(m). \quad (7)$$

This formulation of m_0 is closely related to a path-integral formulation, where the amplitude $|\langle \Psi_0 | \phi_k \rangle|^2$ is the relative amount of time that the system in its ground state will spend in ϕ_k when viewed from our real-space basis.

III. RESULTS

A. Results using order-parameter distribution functions

1. Calculation of the phase boundary

Following an earlier paper,³ we infer the nature and position of the CDW-SDW transition by calculating the CDW order-parameter distribution function, and interpreting it according to the phenomenological theory of Landau. In the thermodynamic limit, the order parame-

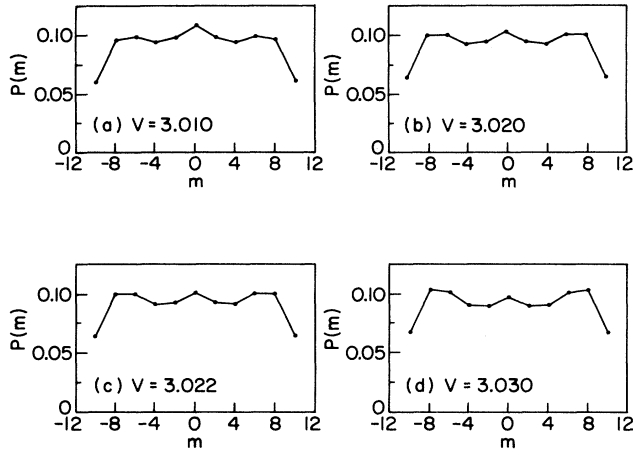


FIG. 1. Distribution of the CDW order parameter obtained by the Lanczos algorithm at $U=5.5$ at various V . Note how the maximum changes from $m=0$ to $m=8$ at approximately 3.022, indicating a first-order transition.

ter will take a value that minimizes the free energy (i.e., the maximum of the measured distribution). To infer the phase boundary we note the values of coupling constants where the maximum of the measured distribution becomes nonzero, and extrapolate to large lattices. In addition, we obtain the nature of the transition by noting whether the order parameter changes continuously (second order) or discontinuously (first order).

To show an example of this, a series of Lanczos-generated CDW order-parameter distributions is shown in Fig. 1. These calculations were made at $N=10$ and $U=5.5$ for various values of V . In Fig. 1(a), calculated at $V=3.0$, the central peak is largest, indicating that the system is not in a CDW state (and is therefore in a SDW state). As V increases, however, the outer peaks increase,

TABLE I. Estimate of the position of the phase boundary at $U=5.5$ using the CDW order-parameter distribution for various values of N , and estimates of the position of the phase boundary at $N=\infty$. The estimates indicate the value of V for which the maximum of the distribution becomes nonzero. The last two rows show the values obtained by extrapolating the measured values to the thermodynamic limit. The terms shown in parentheses are the powers of $1/N$ used to extrapolate to $N=\infty$.

Size	V
12	2.993
10	3.022
8	3.064
6	3.150
$\infty(1,1/N,1/N^2)$	2.892
$\infty(1,1/N^2,1/N^4)$	2.836

TABLE II. Estimate of the position of the phase boundary at $U=3.0$ using the CDW order-parameter distribution for various values of N , and extrapolated to $N=\infty$. The estimates indicate the value of V for which the maximum of the distribution becomes nonzero. The last two rows show the values obtained by extrapolating the measured values to the thermodynamic limit. The terms shown in parentheses are the powers of $1/N$ used to extrapolate to $N=\infty$.

Size	V
12	1.845
10	1.875
8	1.932
6	2.020
$\infty(1,1/N,1/N^2)$	1.685
$\infty(1,1/N^2,1/N^4)$	1.761

and at approximately $V=3.022$ [Fig. 1(c)] there is a discontinuous change in the maximum of $P(m)$, as the two outer maxima exceed the $m=0$ peak. This behavior, if it persists with increasing lattice size, signals a first-order transition. Note the signature of a first-order transition, the characteristic three-peaked distribution, arising from the presence of metastable states.

To estimate the position of the phase boundary, we must extrapolate the position where the maximum of $P(m)$ changes to large N . We do this by performing a least-squares fit of the sequence of estimates to a series in $1/N$. We choose this method of extrapolation, because we expect the finite-size dependence of m to be an analytic function, and therefore to be representable as a series in $1/N$. Since we do not have enough data to find more than a couple of terms of such a series, and we have no *a priori* basis for choosing the powers of $1/N$, we have extrapolated to large N using several different functions of $1/N$, and show the results of two of these here: $f_1(N)=a+b/N+c/N^2$, and $f_2(N)=a+b/N^2+c/N^4$ (a , b , and c are constants). The difference in the numbers obtained with these functions provides a qualitative estimate of the uncertainty. We find that the answers are not sensitive to the choice of function.

Table I shows the sequence of V values where the maximum of the distribution shifts, and estimates of the phase boundary obtained for f_1 and f_2 . The two functions imply a phase transition at $V=2.89$ and 2.93 , respectively. Table II shows the results of similar calculations, performed at $U=3.0$. Our estimated values are 1.68 and 1.76.

2. Position of the tricritical point

As stated earlier, the distribution of m allows us to calculate the position of the tricritical point. To do this, we measure a series of distributions along the indicated phase boundary (the position where the maximum changes), and locate the position where the three-peaked distribution characterizing a first-order transition ap-

pears. Figure 2 shows the results of these calculations for 6, 8, 10, and 12 sites. In Table III we have summarized the indicated nature of the transition for each of the cases we have calculated. Indicated first-order transitions (three-peaked distribution) are labeled with a 1, second-order transitions with a 2, and cases where it is not possible to distinguish between them are indicated with a question mark.

These data show that the indicated position of the tricritical point increases with lattice size. The 6- and 8-site cases, shown in Figs. 2(a) and 2(b), are first order at $U=3.0$, but appear to be second order at $U=2.5$ (consistent with the trend, the $N=8$ data are less strongly first order). The 10-site case is clearly first order at $U=3.5$ and possibly very weakly first order at $U=3.0$, while the 12-site case is second order at $U=3.0$ and possibly at $U=3.5$ (it is definitely first order at $U=4.0$).

Based on this trend, and the fact that our largest case of 12 sites indicates a value in the neighborhood of $U=3.5$, we conclude that the tricritical point occurs above $U=3.5$. Unfortunately, we cannot extrapolate these results to large lattices with any confidence. The relatively large spacing in U between calculations ($\Delta U=0.5$), and the similarity between the two- and

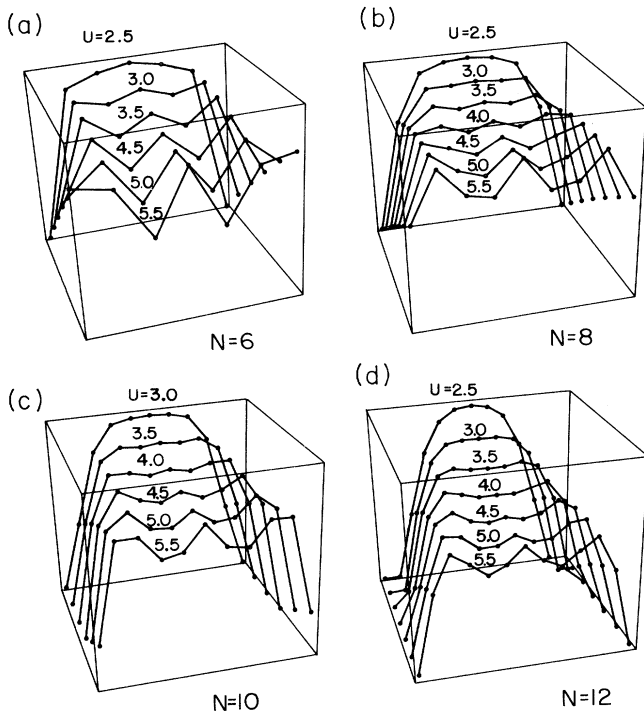


FIG. 2. Variation of the CDW parameter distribution along the phase boundary for various lattice sizes. The point on the phase boundary at which the distributions were calculated are parametrized by U . The appearance of a three-peaked distribution signals a change from a second- to first-order transition. The three-peak distribution appears at larger U for larger lattices, indicating that the actual position of the tricritical point will occur at larger U than observed in these lattices.

TABLE III. Nature of the transition indicated by the distributions shown in Fig. 2 ($U < 5.0$). An apparent first-order transition is denoted by 1, a second-order transition by 2, and a question mark indicates cases where it is not possible to distinguish between the two. Note how the change from first- to second-order behavior occurs at larger values of U as N increases.

N	U				
	2.5	3.0	3.5	4.0	4.5
6	2	1	1	1	1
8	2	1	1	1	1
10	2	?	1	1	1
12	2	2	?	1	1

three-peaked distributions near the tricritical point, make it difficult to precisely locate the positions where the three peaks disappear accurately enough to allow reliable extrapolation. We would assume the consistent increases in the position of the transition from a two-peaked to three-peaked distribution observed in these cases would diminish as lattice size increases, and the position would approach an asymptotic value (possibly between $U=4.0$ and 5.0) for lattice sizes larger than 12 sites, but it is not possible to determine this from the data.

These results confirm the tricritical behavior observed through Monte Carlo simulation. However, the position of the tricritical point indicated by the Lanczos data is higher than the Monte Carlo estimate of $2.5 \leq U \leq 3.0$ (Refs. 1–3) (see Sec. III C). The Lanczos results should be more reliable. They are exact, and even at the small lattice sizes available to us (12 sites) the tricritical point is greater than that indicated by the Monte Carlo data. Because the indicated position of the tricritical point clearly increases as N increases, this is unlikely to be a consequence of our limited lattice size. Rather, it appears that there is a problem with extrapolating the Monte Carlo results to zero temperature and zero $\Delta\tau$. This is somewhat unexpected since this Monte Carlo method is known to reliably calculate ground-state energies.

B. Estimating the phase boundary from finite-size scaling of Lanczos results

We have also used finite-size scaling^{13,14} to obtain an independent estimate of the phase boundary, using scaling of the CDW structure factor, the SDW structure factor, and the method based on cumulants developed by Binder.¹⁵ To see how this works, consider the CDW structure factor (at wave vector $q = \pi$):

$$S_{\text{CDW}} = \frac{1}{N} \sum_{i,l} (-1)^l n_i n_{i+l}. \quad (8)$$

In the ordered state, this quantity is proportional to N , and thus diverges as N increases. Conversely, when we are not in the CDW phase, S_{CDW} must decrease with increasing N to a value determined by the correlation length. Thus at the phase boundary, in the absence of

finite-size effects, there should be a fixed point where S_{CDW} does not depend on N . In practice, finite-size effects modify the scaling so that various pairs of lattice sizes have different fixed points, making it necessary to extrapolate to large N .

Similar arguments also apply for the SDW structure factor and the quantity $g = \frac{1}{2}(3 - \langle m^4 \rangle / \langle m^2 \rangle^2)$ used by Binder. The SDW cannot have true long-range order since it has a continuous symmetry, which by the Mermin-Wagner theorem cannot be broken. However, its correlation functions are long ranged at $T=0$, where these calculations are made, and, therefore, manifest the same behavior as described for the CDW. We find the fact that the method of cumulants can be used here somewhat surprising, considering that the quantity g was derived assuming continuous Gaussian peaks in the distribution function, and is supposed to detect the departure from a Gaussian distribution in a continuous system. This is quite different from the small discrete distributions here ($m = 0, \pm 2, \pm 4, \dots, \pm N$).

Normally, finite-size scaling can also be used to determine the exponents associated with a second-order transition. However, it is not possible here because of the presence of two relevant operators in the neighborhood of the phase boundary. This situation was discussed extensively in Ref. 3.

1. Results using finite-size scaling

Figures 3 and 4 show the results of finite-size scaling calculations at $U=5.5$ and 3.0 for various values of V . In addition, Tables IV and V show the intersections of the scaling parameter versus V curves (the fixed points) in each of the three scaling plots, the quantities that allow us to estimate the fixed point.

Considering the $U=5.5$ S_{CDW} data, we see in Fig. 3(a)

TABLE IV. Finite-size scaling results at $U=5.5$. The table shows the values of V where $S_{\text{CDW}}(\pi)$, $S_{\text{SDW}}(\pi)$, and g , respectively, are equal for lattice sizes N_1 and N_2 (i.e., the fixed points). If there were no finite-size effects, all intersections would occur at the same value of V . Extrapolation of the intersections to large N should eliminate finite-size effects and give the CDW-SDW phase boundary.

N_1	N_2	$S_{\text{CDW}}(\pi)$	$S_{\text{SDW}}(\pi)$	g
12	10	2.803	2.945	2.919
12	8	2.782	2.951	2.926
12	6	2.752	2.962	2.935
12	4	2.716	2.983	2.949
10	8	2.762	2.958	2.935
10	6	2.735	2.972	2.946
10	4	2.697	2.998	2.964
8	6	2.714	2.988	2.957
8	4	2.656	3.021	2.980
6	4	2.609	3.056	3.006

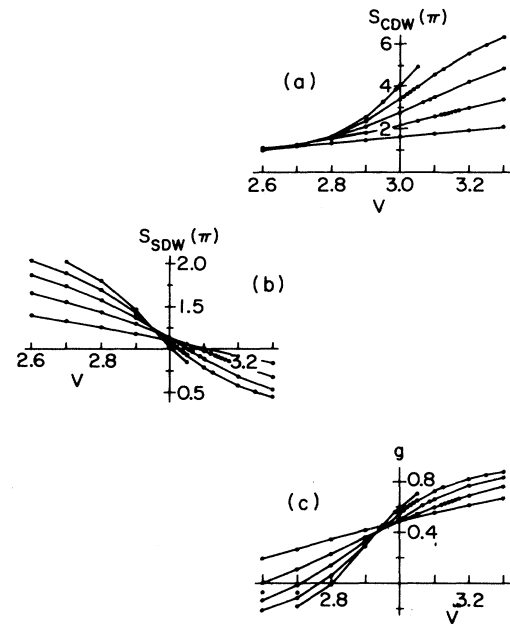


FIG. 3. Finite-sized scaling results obtained at $U=5.5$. The three plots show the CDW structure factor (a), the SDW structure factor (b), and the ratio of cumulants [$g = \frac{1}{2}(3 - \langle m^4 \rangle / \langle m^2 \rangle^2)$] (c) plotted vs V for lattice sizes $N=4, 6, 8, 10$, and 12 . The intersections of the curves, which are used to estimate the phase boundary, are shown in Table IV.

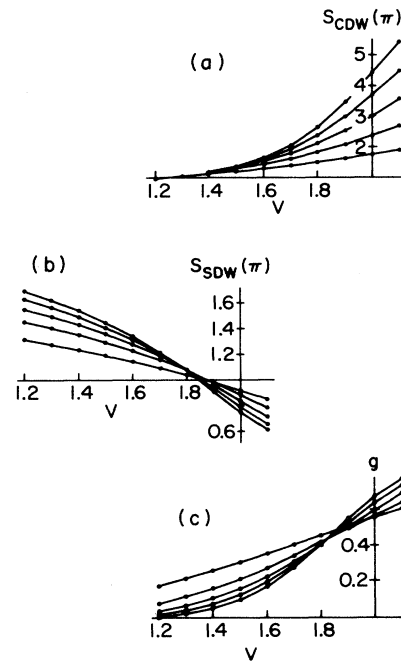


FIG. 4. Finite-sized scaling results at $U=3.0$. The intersections of the curves, which are used to estimate the phase boundary, are shown in Table V.

TABLE V. Finite-size scaling results at $U=3.0$. The table shows the values of V where $S_{\text{CDW}}(\pi)$, $S_{\text{SDW}}(\pi)$, and g , respectively, are equal for lattice sizes N_1 and N_2 (i.e., the fixed points). If there were no finite-size effects, all intersections would occur at the same value of V . Extrapolation of the intersections to large N should eliminate finite-size effects and give the CDW-SDW phase boundary. Note that the $S_{\text{CDW}}(\pi)$ intersections occur at considerably smaller V values. We believe this occurs because the CDW correlation length is larger than the lattices, making finite-size scaling with this parameter less reliable here.

N_1	N_2	$S_{\text{CDW}}(\pi)$	$S_{\text{SDW}}(\pi)$	g
12	10	1.408	1.755	1.766
12	8	1.387	1.770	1.785
12	6	1.351	1.793	1.810
12	4	1.305	1.830	1.851
10	8	1.366	1.784	1.802
10	6	1.334	1.809	1.829
10	4	1.285	1.848	1.874
8	6	1.314	1.828	1.854
8	4	1.258	1.873	1.905
6	4	1.224	1.910	1.952

that the intersections occur at nearly the same point as expected. From column 3 of Table IV, we see that the intersections occur between $V=3.057$ and 2.945 . Again, these values must be extrapolated to large N . Extrapolation using the method of Sec. I indicates a phase boundary between 2.91 and 2.93 . The same procedure performed on the scaling of the $S_{\text{SDW}}(\pi)$ and g indicates a phase boundary between 2.87 and 2.92 [$S_{\text{SDW}}(\pi)$] and between 2.88 and 2.89 (g). These results compare extremely well with the value from the distribution functions, obtained earlier, of between 2.89 and 2.93 . These estimates, and those obtained at $U=3.0$, are shown in Table VI.

At $U=3.0$, extrapolation of the intersections of the $S_{\text{SDW}}(\pi)$ and g curves yield estimates of between 1.65 to 1.69 and 1.61 to 1.70 , respectively (see Table IV). Once again, these values are consistent with the results obtained from the CDW order-parameter distribution (between 1.69 and 1.76). The greater spread in these numbers reflects the fact that the transition is not as sharp at $U=3$, which we have estimated to be below the tricritical point (and therefore continuous rather than discontinuous as at $U=5.5$).

ous as at $U=5.5$).

The $S_{\text{CDW}}(\pi)$ estimates are lower (1.48 to 1.59). We believe the reason for this is that the CDW correlation length is greater than the size of our lattice. In this situation, we may be measuring the point at which the correlation length exceeds the lattices we are working with, which may not be close to the phase boundary. This should be expected to occur more strongly for the CDW scaling than the SDW scaling because the CDW has a discrete symmetry, and is therefore stiffer against fluctuations than the SDW, which has a continuous symmetry. Considering that the $S_{\text{CDW}}(\pi)$ curve intersections, shown in Table V, column 3, occur between 1.2 and 1.4 , compared with $V=1.75$ to 1.95 for $S_{\text{SDW}}(\pi)$ and g , it is remarkable that the CDW estimate differs by only 15% from the other estimates. The consistency of these numbers, despite the differences in raw data, provides evidence for the reliability of our extrapolation to larger lattice sizes.

C. Comparison of Lanczos and Monte Carlo results

In an earlier paper,³ two of us reported the results of Monte Carlo simulations using the ‘‘checkerboard breakup’’ method of simulating fermions in one spatial dimension. Our conclusion in this paper was that the tricritical point occurred at approximately $U=1.5$. Since submission of the paper, we have performed additional Monte Carlo simulations. We have found that the value of $\Delta\tau$ used for the calculations was too large (0.5), resulting in systematic errors. While the tricritical phenomena persist, the indicated position of the tricritical point increases as $\Delta\tau$ decreases. Unfortunately, we find that low acceptance rates for calculations with small $\Delta\tau$ and large inverse temperature (β), combined with the presence of metastable states, make reliable calculation of the order-parameter distribution function difficult, and hinder systematic extrapolation to large N . Calculations on lattice sizes of 8 , 16 , and 24 sites with $\Delta\tau$ as low as 0.125 show that, at constant β , the indicated position of the tricritical point increases as $\Delta\tau$ decreases and as lattice size increases. While extrapolation of these numbers is problematic, they indicate a tricritical point between $U=2.5$ and 3.0 . Note that even for the largest lattice, $N=24$, the Monte Carlo data are still significantly lower than that indicated by the exact Lanczos calculations. Since both Monte Carlo and Lanczos results show that the in-

TABLE VI. Summary of estimates of CDW-SDW phase boundary at $U=5.5$ and 3.0 . The numbers in parentheses give the range of possible V values estimated by each method. The column labeled m_{CDW} was obtained from the CDW order-parameter distribution function (see Sec. III A), and finite-size scaling of S_{CDW} , S_{SDW} , and the quantity g developed by Binder (see Ref. 15).

U	$S_{\text{CDW}}(\pi)$	$S_{\text{SDW}}(\pi)$	g	m_{CDW}
5.5	(2.907,2.915)	(2.919,2.924)	(2.878,2.888)	(2.926,2.944)
3.0	(1.572,1.596)	(1.655,1.656)	(1.605,1.647)	(1.750,1.623)

licated tricritical point increases with increasing lattice size, it appears that the Monte Carlo results have not converged to the low-temperature, small- $(\Delta\tau)$ limit.

IV. SUMMARY

We have calculated the position of the CDW-SDW phase boundary and the tricritical point of the one-dimensional extended Hubbard model using the Lanczos algorithm. Estimates of the phase boundary using the CDW order-parameter distribution functions, and finite-size scaling of the CDW and SDW structure factors and g yield consistent answers. We estimate the phase boundary to occur at roughly $V=2.92\pm 0.04$ at $U=5.5$ and $V=1.65^{+0.10}_{-0.05}$ at $U=3.0$. The uncertainties reflect the range of values indicated by the various methods we have used rather than a statistical confidence level. Through use of the CDW order-parameter distribution function we estimate the tricritical point to occur above $U=3.5$ and possibly as high as $U=5.0$ although we were not

able to establish the upper bound with confidence.

The accuracy of the Lanczos calculations provides a complementary technique to earlier Monte Carlo calculations, which can be performed on larger lattices. We find extrapolation to the thermodynamic limit to be more reliable with the Lanczos numbers despite the small lattices that are accessible to us. This is due to the fact that in addition to extrapolating to large lattices, the Monte Carlo data must also be extrapolated to low temperature, and small $\Delta\tau$.

ACKNOWLEDGMENTS

This work was supported in part by NSF Grants No. DMR-86-12860/24 and No. DMR-88-18713. We would like to thank the staff of the University of Illinois Materials Research Laboratory Center for Computation and the National Center for Supercomputing Applications (NCSA) for their assistance. The calculations were performed in part on the NCSA Cray-2.

*Present address: Department of Physics and Astronomy, Calvin College, Grand Rapids, MI 49502-6054.

¹J. E. Hirsch, Phys. Rev. B **31**, 6022 (1985).

²J. E. Hirsch, Phys. Rev. Lett. **53**, 2327 (1984).

³J. W. Cannon and E. Fradkin, Phys. Rev. B **41**, 9435 (1990).

⁴V. J. Emery, in *Highly Conducting One-Dimensional Solids*, edited by J. T. Devreese, R. P. Evrard, and V. E. van Doren (Plenum, New York, 1979).

⁵D. Cabib and E. Callen, Phys. Rev. B **12**, 5249 (1975).

⁶B. Fourcade and Spronken, Phys. Rev. B **29**, 5089 (1984).

⁷B. Fourcade and Spronken, Phys. Rev. B **29**, 5099 (1984). This made use of Lanczos calculations, though the approach is quite different from that presented here.

⁸J. E. Hirsch, D. J. Scalapino, R. L. Sugar, and R. Blanken-

becler, Phys. Rev. B **26**, 5033 (1982).

⁹R. Jullien and R. M. Martin, Phys. Rev. B **26**, 6173 (1982).

¹⁰James Hardy Wilkinson, *The Algebraic Eigenvalue Problem* (Oxford University Press, Oxford, 1982).

¹¹R. Whitehead, A. Watt, B. J. Cole, and I. Morrison, *Computational Methods for Shell-Model Calculations*, Advances in Nuclear Physics Vol. 9 (Plenum, New York, 1977), p. 123.

¹²E. Dagotto and A. Moreo, Phys. Rev. D **31**, 865 (1986); E. Gagliano, E. Dagotto, A. Moreo, and F. Alcaraz, Phys. Rev. B **34**, 1677 (1986); **35**, 5297 (1987).

¹³W. L. McMillan, Phys. Rev. B **29**, 4026 (1984).

¹⁴M. P. Nightingale, J. Appl. Phys. **53**, 7927 (1982).

¹⁵K. Binder, Z. Phys. B **43**, 119 (1981); J. Comp. Phys. **59**, 1 (1985).